

DSS-13 Beam-Waveguide Antenna Performance in the Bypass Mode

S. R. Stewart

Ground Antennas and Facilities Engineering Section and PRC, Inc., Pasadena, California

A new 34-meter beam-waveguide (BWG) antenna that contains two microwave paths, a centerline feed system, and a bypass feed system, has been built at Deep Space Station 13 (DSS 13) at Goldstone, California. Previous articles have described the test results from the evaluation of the centerline BWG feed system in the receive mode as well as the test package hardware used to perform these tests [1-5]. This article presents the test results from the evaluation of the bypass BWG feed system on the DSS-13 antenna in the receive mode, including the operating noise-temperature and the antenna-area-efficiency measurements.

I. Introduction

The new 34-meter beam-waveguide (BWG) antenna, which was built at DSS 13, was designed with two BWG receiver paths: a centerline feed system, which terminates in the pedestal room at the f3 focal point, and a bypass feed system, which terminates on the alidade structure at the f4 focal point (Fig. 1). The centerline feed system has already been evaluated for zenith operating noise-temperature and antenna-area-efficiency performance at X-band (8.45 GHz) and Ka-band (32 GHz) at the two focal points, f1 and f3 [1]. The bypass BWG feed system has now been evaluated at both X-band and Ka-band. In order to maintain consistency, the same test packages that were used to evaluate the centerline feed BWG system were used to test the bypass BWG feed system [2-6].

II. Initial Measurements

Some initial testing at the f4 focal point was conducted to ensure that the receiver equipment was working

properly and that the four mirrors in the bypass system were aligned properly. The X-band test package with its 29-dBi horn was installed at the f4 focal point (Fig. 2) and antenna-efficiency and noise-temperature measurements were immediately begun. Based on previous measurements at f1 and f3 in the centerline-feed BWG mode [1], it was estimated that a well-aligned BWG feed system would result in a peak antenna-aperture efficiency of at least 70 percent near 45 deg elevation. The preliminary data, however, showed a distorted antenna pattern with a peak antenna efficiency of 66 percent at 70 deg elevation. In an effort to find the cause of this problem, the test package was removed and theodolite measurements of the alignment of the mirrors in the bypass feed system were repeated with the antenna at 45 deg elevation. The alignment and positions of the two paraboloid mirrors and the lower flat mirror relative to each other and relative to the shroud walls were verified to be correct to within ± 0.40 cm from their design positions and ± 0.02 deg from their design angles with the antenna at 45 deg elevation. The position and angle of the upper flat mirror and the relative position

between the upper paraboloid and flat mirrors were verified with the antenna at zenith. The measurements that could not be made, however, were the changes in relative position between the mirrors due to flexure in the antenna structure as the antenna moves in elevation.

Knowing that all of the hardware was positioned correctly, a detailed investigation of the antenna's performance was begun by measuring its far-field pattern. The high signal-to-noise ratio of the 12.198-GHz beacon on board a geostationary satellite was required for accurate antenna-pattern measurements, so a Ku-band (12.198-GHz) receiver system [6] was installed at f4. Antenna-pattern measurements were made that indicated a substantial misalignment in the mirrors relative to their optimum positions (Fig. 3).

A full analysis of the alignment errors contributed by each of the four mirrors would have seriously delayed this work, so it was decided to move the most sensitive mirror until the antenna pattern, with the antenna near 45 deg elevation, was balanced and then proceed with the antenna-efficiency measurements even though it was known that movement of just one mirror would not yield the optimum operating noise temperature and antenna gain.

Communication with D. Bathker and W. Veruttipong¹ indicated that the paraboloid mirror on the dish surface was the most sensitive. Movements of both 0.193 deg about the mirror's x-axis and 0.255 deg about the y-axis were required to balance the antenna pattern (Figs. 4 and 5). The cause for this discrepancy between the optical alignment and the RF alignment is presumed to be at least partially due to flexure in the antenna between the 45- and 90-deg elevation angles, where the mirror alignments were checked. After the alignment was complete, the X-band test package was reinstalled at f4 and operating noise-temperature and antenna-efficiency measurements resumed.

III. Measurement Techniques

Throughout this experiment, two radiometer programs were relied on for maximizing the antenna performance measurements. The software is almost identical to that which was used during the testing of the centerline BWG system, with a few minor modifications and improvements. The first software package is the automatic bore-sight program, AUTOBORE, which measures the radio-source noise temperature and calculates antenna pointing

errors by making a continuous series of five-point bore-sights on a given source throughout a 12-hour track. This software has been described in detail elsewhere [1,4], and some parts are reproduced below.

The second package is the calibration software, which is used to measure the gain stability, amplifier linearity, and operating temperature of the system over long periods of time by making calibration measurements periodically and recording these data to disk. The receiver is calibrated by measuring the detected noise power with the receiver in four different configurations: the receiving path of the waveguide switch turned to the feed horn, the receiving path turned to a waveguide ambient load, and each of these configurations with an injected noise-diode signal. A power measurement with the power meter terminated into a 50- Ω load and a physical temperature measurement of the ambient load are also made and added to a disk file. Calculations of the system gain based on the known temperature and noise-power output of the waveguide ambient load are made and used to determine the current operating noise temperature. Evaluation of system linearity is made by comparing the noise power injected by the diode in each of the waveguide configurations. These calibrations are made automatically every 30 minutes or at any other user-defined time interval.

IV. Test Results

A. X-Band Zenith Noise-Temperature Measurements

The X-band test package with its 29-dBi horn was used to make comparative zenith operating noise-temperature measurements at two locations: on the ground and on the antenna at the f4 focal point. Continuous measurements at each of these locations were conducted over two-day periods, with operating noise-temperature (T_{op}) measurements being made every 30 minutes and ambient weather conditions, including temperature, pressure, and relative humidity (RH), being measured every 10 minutes. Figures 6(a) and (b) contain typical calibration data that were collected with the X-band test package on the ground, and Figs. 7(a) and (b) contain calibration data collected at f4, with the antenna at the zenith position. These calibration plots are included to exemplify the stability of the system during the measurement period. Since each of the operating noise temperatures was calculated using the most recent gain factor, corrections for gain changes were automatically accounted for. Corrections for system nonlinearity, however, were not made since the magnitude of the linearity factor is on the order of its uncertainty at ± 1 percent and making any corrections for this factor would have only a minor effect. Table 1 shows the compiled results

¹ Private communications with D. Bathker and W. Veruttipong of the Jet Propulsion Laboratory on 11 April 1991 and 19 April 1991.

would have only a minor effect. Table 1 shows the compiled results of the X-band T_{op} measurements, as well as the weather conditions present during the observation period. Table 1 also shows the corrections that were made to the operating noise-temperature measurements in order to normalize them to the weather conditions present during an average Goldstone day. This normalized T_{op} was computed from

$$T_{op,n} = T_{op} + (T'_{cb}/L_{wg})(1/L_{atm,s} - 1/L_{atm}) \\ + (1/L_{wg})(T_{atm,s} - T_{atm}) + (T_{wg,s} - T_{wg}) \quad (1)$$

where T_{atm} and T_{wg} are, respectively, the atmospheric and waveguide noise-temperature contributions, and L_{atm} and L_{wg} are the atmospheric and waveguide loss factors.

Values for the standard DSS-13 atmospheric conditions² at 8.45 GHz are

$$T_{atm,s} = 2.17 \text{ K}$$

$$L_{atm,s} = 1.00814 \text{ (corresponding to 0.0352 dB)}$$

Other X-band values used for the above equation are

$$T'_{cb}{}^3 = 2.5 \text{ K}$$

$$L_{wg} = 1.0163 \text{ (corresponding to 0.07 dB)}$$

$$T_{wg,s} = 4.69 \text{ K for the above } L_{wg} \text{ and a standard physical waveguide temperature of } 20 \text{ deg C}$$

By normalizing the T_{op} measurements, it is easier to compare these measurements with each other as well as with those made at any other time of the year. As a means of comparison between these results for f4 and the results obtained previously for f1 and f3, Table 2 contains a summary of some differential zenith operating noise temperatures. All of the T_{op} values presented in Table 2 have been normalized to standard DSS 13 atmospheric conditions at 8.45 GHz.

B. X-Band Antenna-Efficiency Measurements

The antenna's efficiency performance is determined by continuously tracking a stellar radio source and measur-

ing the peak received noise power in relation to the background atmospheric noise over a full 10–12 hour track. By knowing the maximum signal strength of the radio source, the aperture efficiency with respect to the elevation angle of the antenna can be determined.

During X-band testing, eight full days of antenna-efficiency measurements were conducted, using the four radio sources that are listed and described in Table 3. Two of these sources are constant and well calibrated while the other two are variable. The two variable sources are good for relative measurements over a short period of days, but need to be calibrated against known, stable sources. Therefore, Table 4 contains the correction factors which needed to be applied to the variable sources in order to make them useful. Figure 8 shows the combined antenna efficiency measurements at X-band versus elevation angle for the f4 focal point with the effects of atmospheric attenuation removed. An average antenna efficiency with a peak of 71.4 percent at an elevation angle of 38.6 deg is also shown in this figure.

C. Ka-Band Zenith Noise-Temperature Measurements

As with X-band, the Ka-band test package with its 29-dBi horn was used to make comparative zenith T_{op} measurements on the ground and on the antenna at the f4 focal point (Fig. 9). Continuous measurements at each of these locations were made over two-day periods, with operating noise-temperature measurements being taken every 30 minutes and ambient weather conditions being measured every ten minutes. Figures 10(a) and (b) contain typical calibration data that were collected with the Ka-band test package on the ground, and Figs. 11(a) and (b) contain typical calibration data collected at f4, with the antenna at the zenith position. As with the X-band measurements described above, corrections for gain changes are already accounted for in the operating noise-temperature measurements, and no corrections were made for linearity which would have an effect of less than ± 2 percent.

Table 1 shows the compiled results of the Ka-band T_{op} measurements, as well as the weather conditions present during the observation period. The normalized T_{op} values, which were calculated using Eq. (1), are also included in this table, for comparison purposes.

Values for the standard DSS-13 atmospheric conditions at 32 GHz are

$$T_{atm,s} = 7.02 \text{ K}$$

$$L_{atm,s} = 1.02683 \text{ (corresponding to 0.1150 dB)}$$

² Deep Space Network/Flight Project Interface Design Handbook, Document 810-5, Rev. D, vol. I, sec. TCI-30 (internal document), Jet Propulsion Laboratory, Pasadena, California, June 1, 1990.

³ T'_{cb} is the effective noise contribution from cosmic background radiation. This value is a function of frequency and will differ from the nominal noise temperature of 2.7 K.

Other Ka-band values used for Eq. (1) are

$$T'_{cb} = 2.0 \text{ K}$$

$$L_{wg} = 1.06414 \text{ (corresponding to 0.27 dB)}$$

$$T_{wg,s} = 17.67 \text{ K for the above } L_{wg} \text{ and a standard physical waveguide temperature of } 20 \text{ deg C}$$

Table 2 contains a comparison between these results for f4 and the results obtained previously for f1 and f3. This comparison may be slightly erroneous due to the six-month time lapse between measurements. All of the T_{op} values presented in Table 2 have been normalized to standard DSS-13 atmospheric conditions at 32 GHz.

D. Ka-Band Antenna-Efficiency Measurements

During Ka-band testing, eight full days of antenna-efficiency measurements were conducted using four radio sources. These four sources are listed and described in Table 5. The flux densities of two sources, 3C 274 and Venus, have been thoroughly measured at 32 GHz, but those of the other two sources have not. In addition, flux values from Venus are continually changing due to the change in Venus's position relative to the Earth, and must be updated daily. The two variable sources that were used (3C 84 and 3C 273) had to have their flux

values corrected against the calibrated sources, and these corrections are found in Table 6. Figure 12 shows the combined antenna-efficiency measurements versus elevation angle for Ka-band at the f4 focal point, with the effects of atmospheric attenuation removed. An average antenna-efficiency having a peak of 45.0 percent at an elevation angle of 41.4 deg is also shown in this figure. The standard deviation of these data points is 5.0 percent.

Figure 13 contains the combined results of antenna-efficiency measurements at both X-band and Ka-band for the three focal points, f1, f3, and f4. The results shown in this figure, like those in Figs. 8 and 12, have had the effects of atmospheric attenuation removed.

V. Conclusions

The bypass feed system of the DSS-13 BWG antenna has been fully tested for noise-temperature and antenna-efficiency performance at both X-band and Ka-band. The mirror movements inside the beam waveguide that were necessary in order to make adequate measurements of these parameters resulted in a bypass feed system which may be slightly less than optimal. The results, however, show a system whose performance at both 8.45 and 32 GHz at the bypass focal point, f4, is consistent with those at f1 and f3.

Acknowledgments

The assistance of DSS-13 personnel G. Bury, J. Crook, L. Smith, R. Reese, J. Garnica, G. Farner, and R. Littlefair is gratefully acknowledged. The author also thanks DSS-13 group supervisor, C. Goodson, and the DSS-13 station manager, A. Price, for their continual support throughout the measurement process.

References

- [1] S. D. Slobin, T. Y. Otoshi, M. J. Britcliffe, L. S. Alvarez, S. R. Stewart, and M. M. Franco, "Efficiency Calibration of the DSS 13 34-Meter Diameter Beam Waveguide Antenna at 8.45 and 32 GHz," *TDA Progress Report 42-106*, vol. April-June 1991, Jet Propulsion Laboratory, Pasadena, California, pp. 283-297, August 15, 1991.
- [2] T. Y. Otoshi, S. R. Stewart, and M. M. Franco, "A Portable X-Band Front-End Test Package for Beam-Waveguide Antenna Performance Evaluation—Part I: Design and Ground Tests," *TDA Progress Report 42-103*, vol. July-September 1990, Jet Propulsion Laboratory, Pasadena, California, pp. 135-150, November 15, 1990.
- [3] T. Y. Otoshi, S. R. Stewart, and M. M. Franco, "A Portable X-Band Front-End Test Package for Beam Waveguide Antenna Performance Evaluation—Part II: Tests on the Antenna," *TDA Progress Report 42-105*, vol. January-March 1991, Jet Propulsion Laboratory, Pasadena, California, pp. 54-68, May 15, 1991.
- [4] T. Y. Otoshi, S. R. Stewart, and M. M. Franco, "A Portable Ka-Band Front-End Test Package for Beam Waveguide Antenna Performance Evaluation—Part I: Design and Ground Tests," *TDA Progress Report 42-106*, vol. April-June 1991, Jet Propulsion Laboratory, Pasadena, California, pp. 249-265, August 15, 1991.
- [5] T. Y. Otoshi, S. R. Stewart, and M. M. Franco, "A Portable Ka-Band Front-End Test Package for Beam Waveguide Antenna Performance Evaluation—Part II: Tests on the Antenna," *TDA Progress Report 42-106*, vol. April-June 1991, Jet Propulsion Laboratory, Pasadena, California, pp. 266-282, August 15, 1991.
- [6] T. Y. Otoshi, S. R. Stewart, and M. M. Franco, "A Portable Ku-Band Front-End Test Package for Beam Waveguide Antenna Performance Evaluation," *TDA Progress Report 42-107*, vol. July-September 1991, Jet Propulsion Laboratory, Pasadena, California, pp. 73-80, November 15, 1991.

Table 1. Measured zenith operating noise temperatures corrected for weather and waveguide-loss changes for X-band and Ka-band.

Configuration	Observation period, UT	Average measured T_{op} , K	Average weather during observation	Computed T_{atm} , K	Computed L_{atm}	Physical waveguide temp., deg C	T_{wg} , K	Normalized T_{op} , K
X-band, on the ground	03/12/91 1600 03/13/91 1730	22.29	893.6 mbar 8.9 deg C 37.3% RH	2.25	1.0085 (0.037 dB)	13.34	4.58	22.32
X-band, at f4	04/27/91 0500 04/28/91 2030	28.84	891.3 mbar 17.6 deg C 26.4% RH	2.27	1.0086 (0.037 dB)	13.96	4.59	28.84
Ka-band, on the ground	04/23/91 1200 04/24/91 2330	83.09	890.8 mbar 9.96 deg C 69.9% RH	10.94	1.0418 (0.178 dB)	5.05	16.77	80.33
Ka-band, at f4	05/11/91 0030 05/12/91 2230	93.51	894.1 mbar 12.6 deg C 34.4% RH	8.22	1.0312 (0.133 dB)	7.65	16.93	93.13

Table 2. Differential zenith operating noise temperatures at X-band.

Configurations differenced	X-band delta T_{op} , K	Ka-band delta T_{op} , K
F1–Ground	3.2 ^a	7.1 ^b
F2–F1	—	5.2 ^b
F3–F1	8.9 ^a	6.8 ^b
F4–F1	3.3	5.7
F2–Ground	—	12.3
F3–Ground	12.1	13.9
F4–Ground	6.5	12.8

^a These values obtained from [3].
^b These values obtained from [5].

Table 3. Radio sources used for X-band calibrations at f4, April 1991. (The values below were obtained from [1].)

Source	Declination, J2000.0	Peak elevation at DSS 13	Flux, Jy	C_r	T_{100}/C_r , K
3C 274	12.391	67.1	44.555	1.087	13.477
3C 123	29.671	84.4	9.404	1.0054	3.075
3C 84	41.512	83.7	45.79	1.000	15.056
3C 273	2.052	56.8	36.46	1.000	11.988

Table 4. Efficiency adjustments, deduced flux, and T100/C_r values for X-band at f4, April 1991.

Source	Efficiency adjustment needed	Deduced flux, Jy	Deduced T100/C _r , K
3C 274 ^a	1.000	44.555	13.477
3C 123 ^b	0.98558	9.542	3.12
3C 84 ^c	1.43801	31.843	10.47
3C 273 ^c	1.17529	31.022	10.20

^a Constant, extended.
^b Constant, nonpoint.
^c Variable, point.

Table 5. Radio sources used for Ka-band calibrations at f4, May 1991.

Source	Declination, J2000.0	Distance, AU	Peak elevation at DSS 13	Flux, Jy	C _r	T100/C _r , K
3C 274 ^a	12.391		67.1	16.22	1.2730	4.190
3C 84 ^a	41.512		83.7	43.71	1.0000	14.372
3C 273 ^a	2.052		56.8	29.54	1.0000	9.713
Venus 1991 ^b						
01 May	+25.3	1.0511	80.0	71.085	1.0254	22.804
10 May	+25.9	0.9842	80.6	81.076	1.0290	25.918
20 May	+25.5	0.9072	80.2	95.430	1.0342	30.353

^a Values obtained from [1].

^b Declination of date.

Table 6. Efficiency adjustments, deduced flux, and T100/C_r values for Ka-band at f4, May 1991.

Source	Efficiency adjustment needed	Deduced flux, Jy	Deduced T100/C _r , K
3C 274 ^a	0.98172	16.52	4.268
Venus ^b	1.0000	See Table 5	See Table 5
3C 84 ^c	1.45687	30.003	9.865
3C 273 ^c	0.62867	46.987	15.45

^a Constant, extended.

^b Ephemeris dependent, nonpoint.

^c Variable, point.

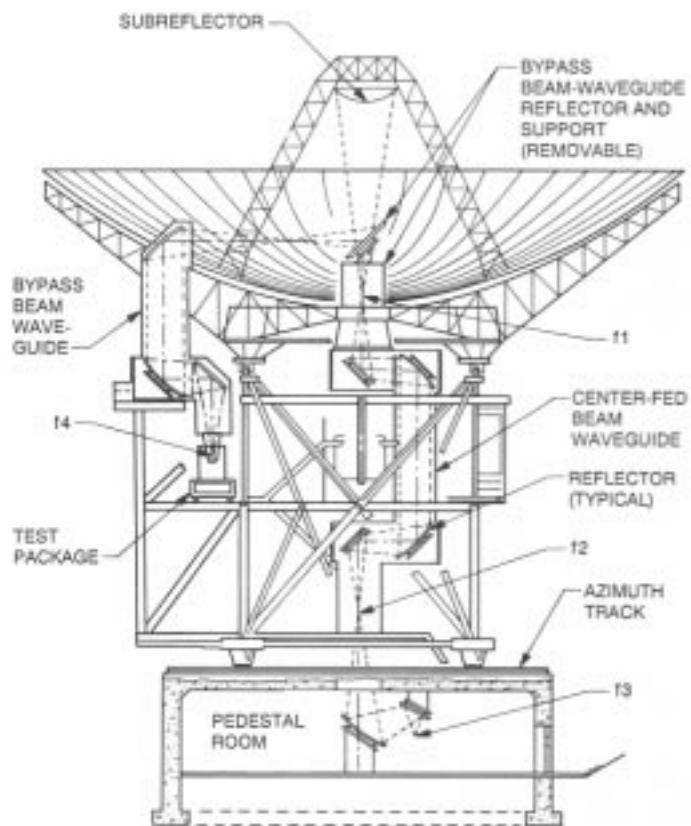


Fig. 1. DSS-13 beam-waveguide antenna depicting focal points f_1 , f_3 , and f_4 .



Fig. 2. X-band test package with its 29-dBi horn being lifted into position at the f_4 focal point.

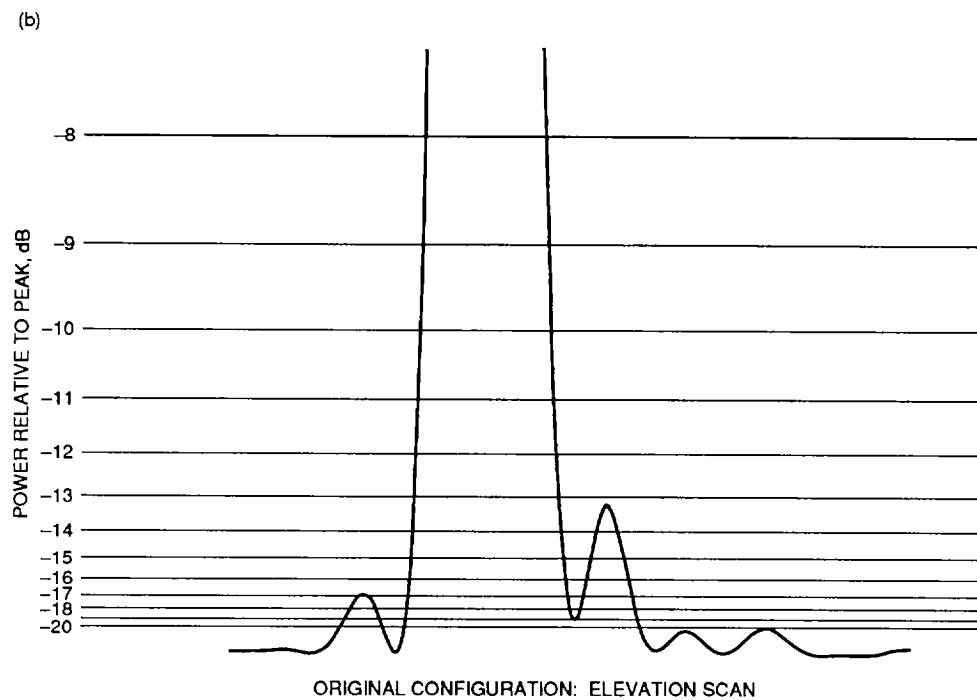
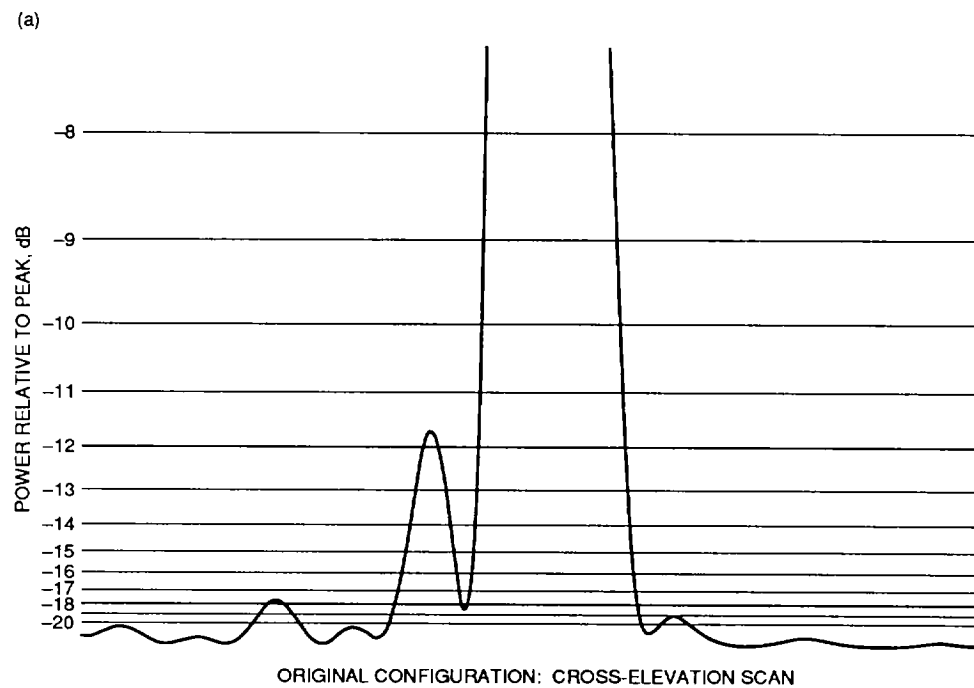


Fig. 3. Antenna pattern before mirror alignment: (a) In the cross-elevation axis and (b) in the elevation axis.

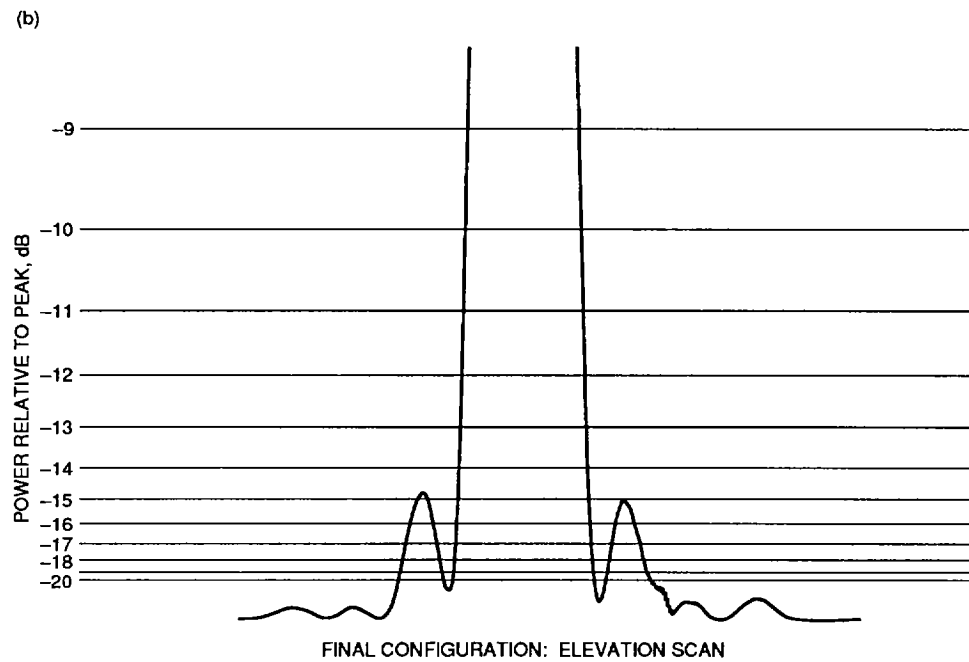
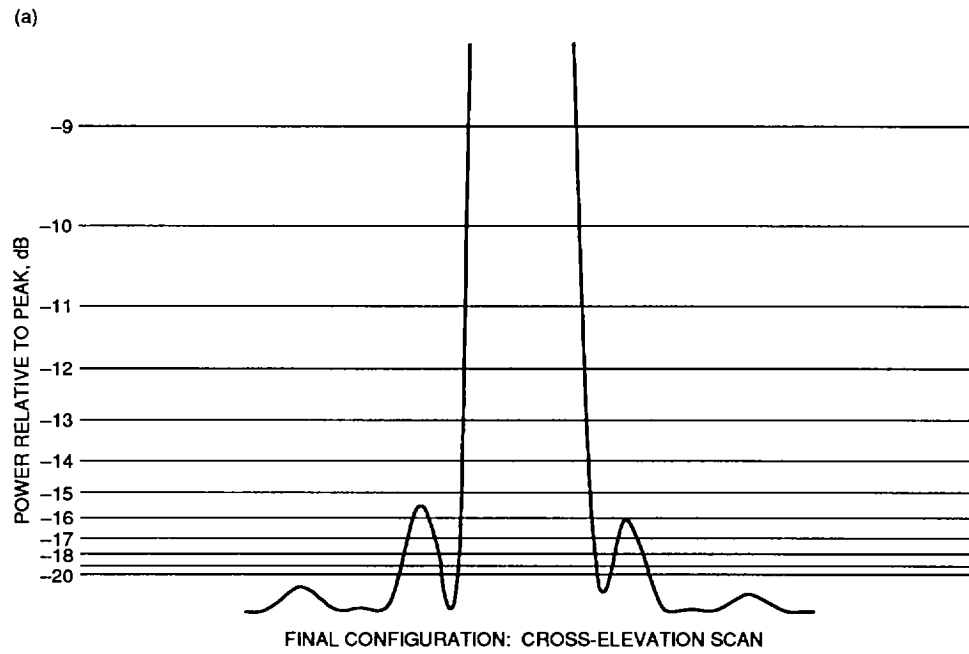


Fig. 4. Antenna pattern after mirror alignment: (a) In the cross-elevation axis and (b) in the elevation axis.

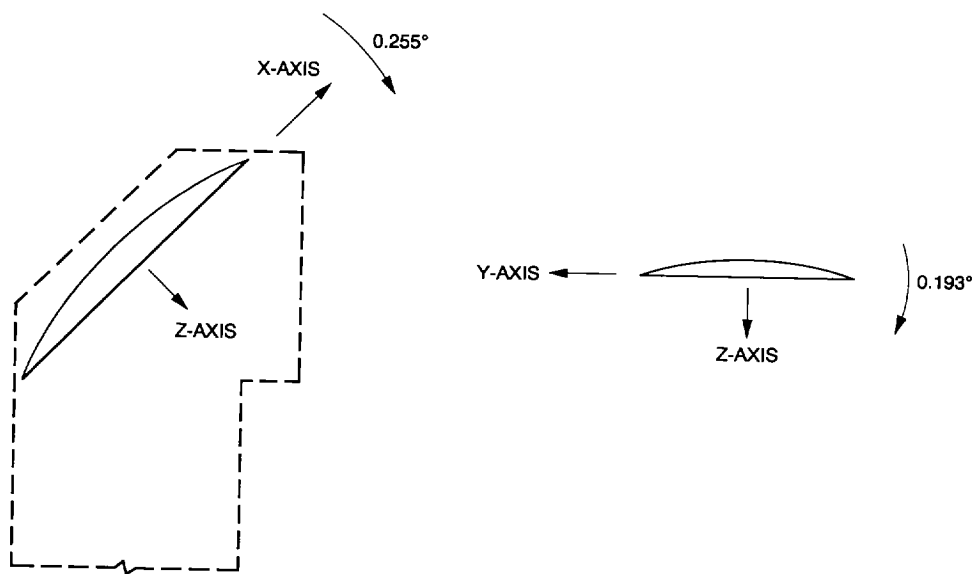


Fig. 5. Motion of upper parabolic mirror.

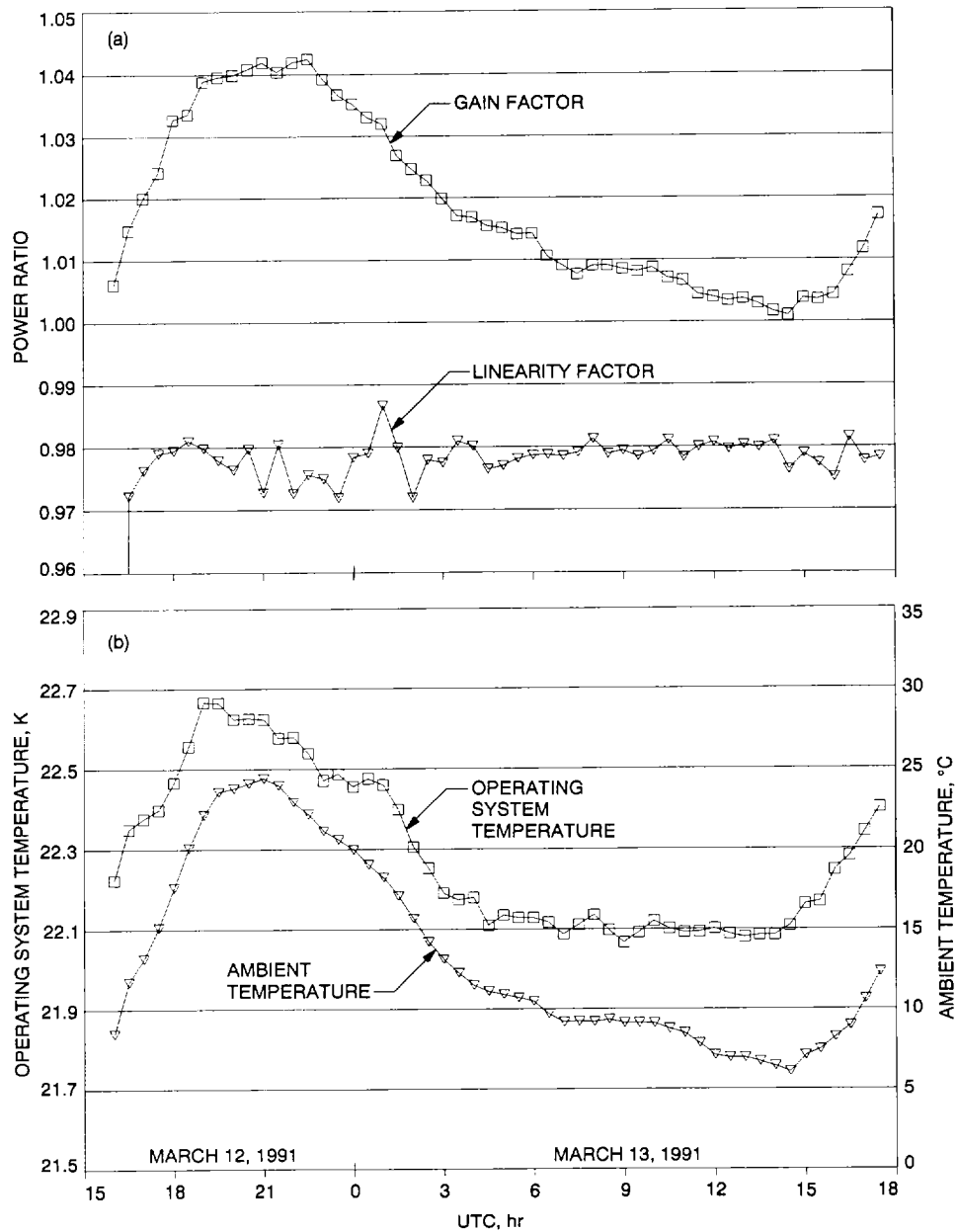


Fig. 6. X-band zenith noise-temperature measurements on the ground: (a) system gain and linearity and (b) system temperature.

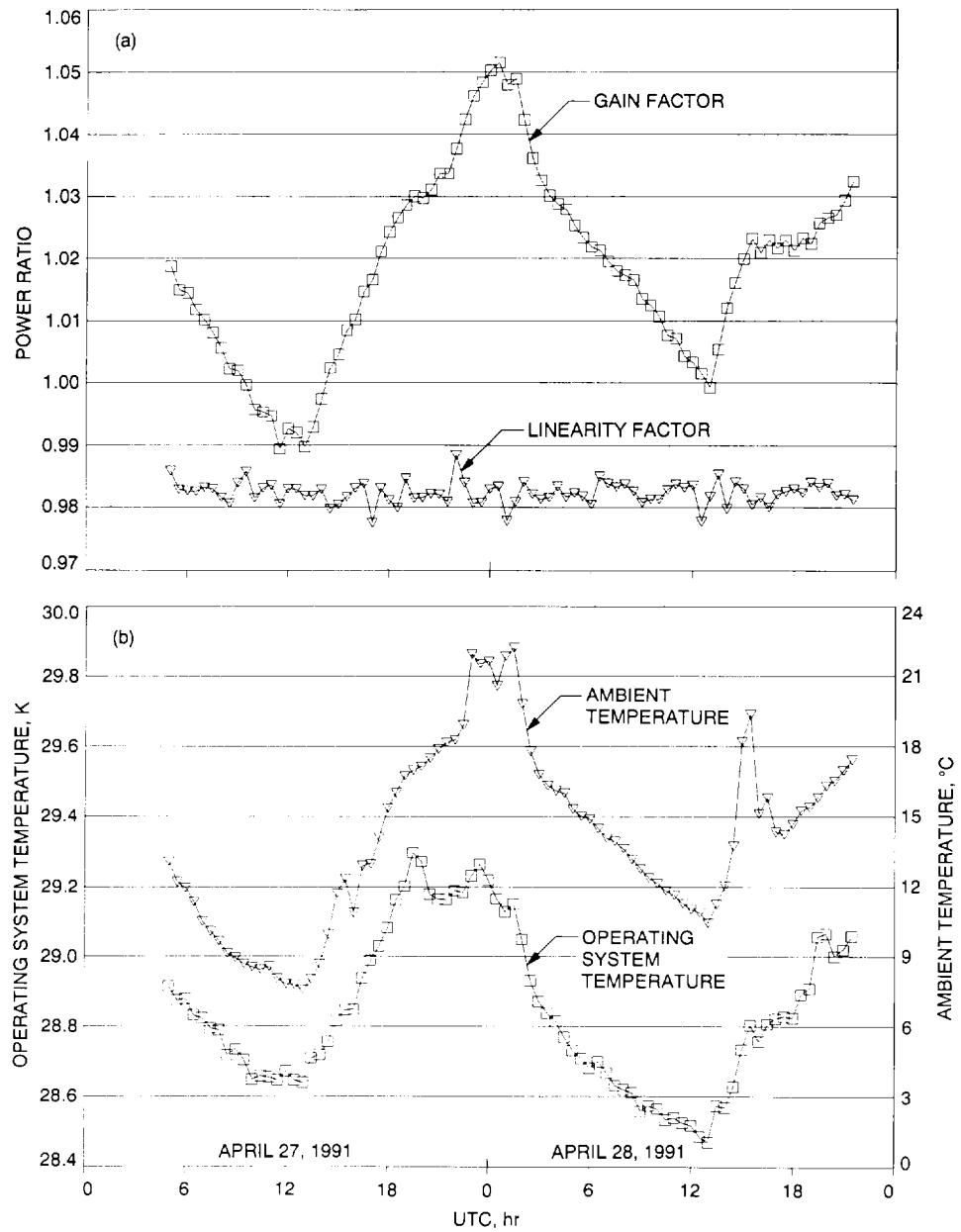


Fig. 7. X-band zenith noise-temperature measurements on the antenna: (a) system gain and linearity and (b) system temperature.

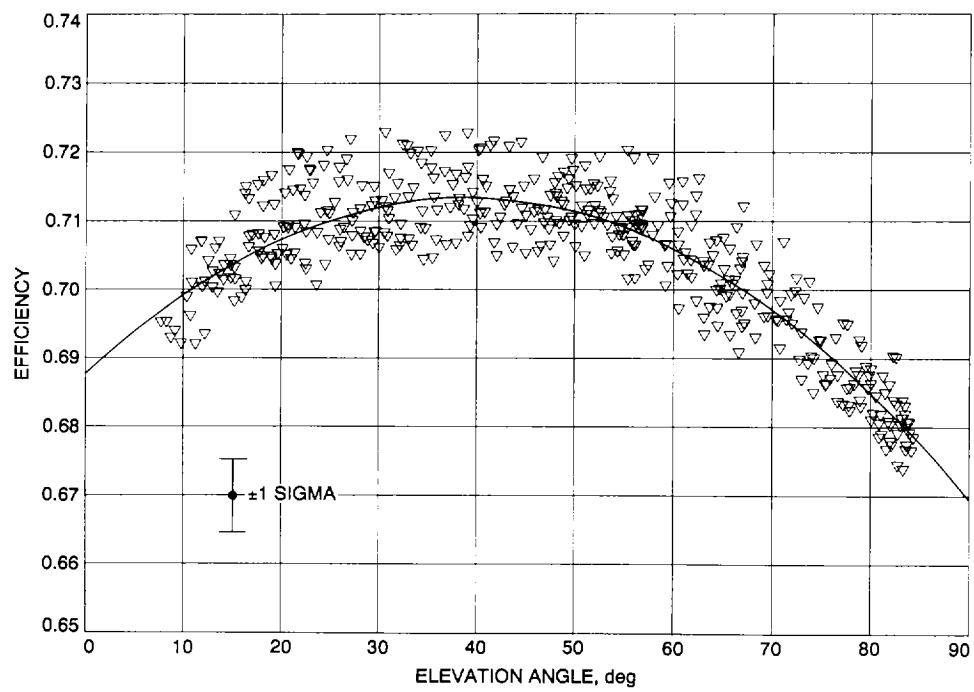


Fig. 8. X-band efficiency plot.



Fig. 9. Ka-band test package with 29-dBi horn at the f4 focal point.

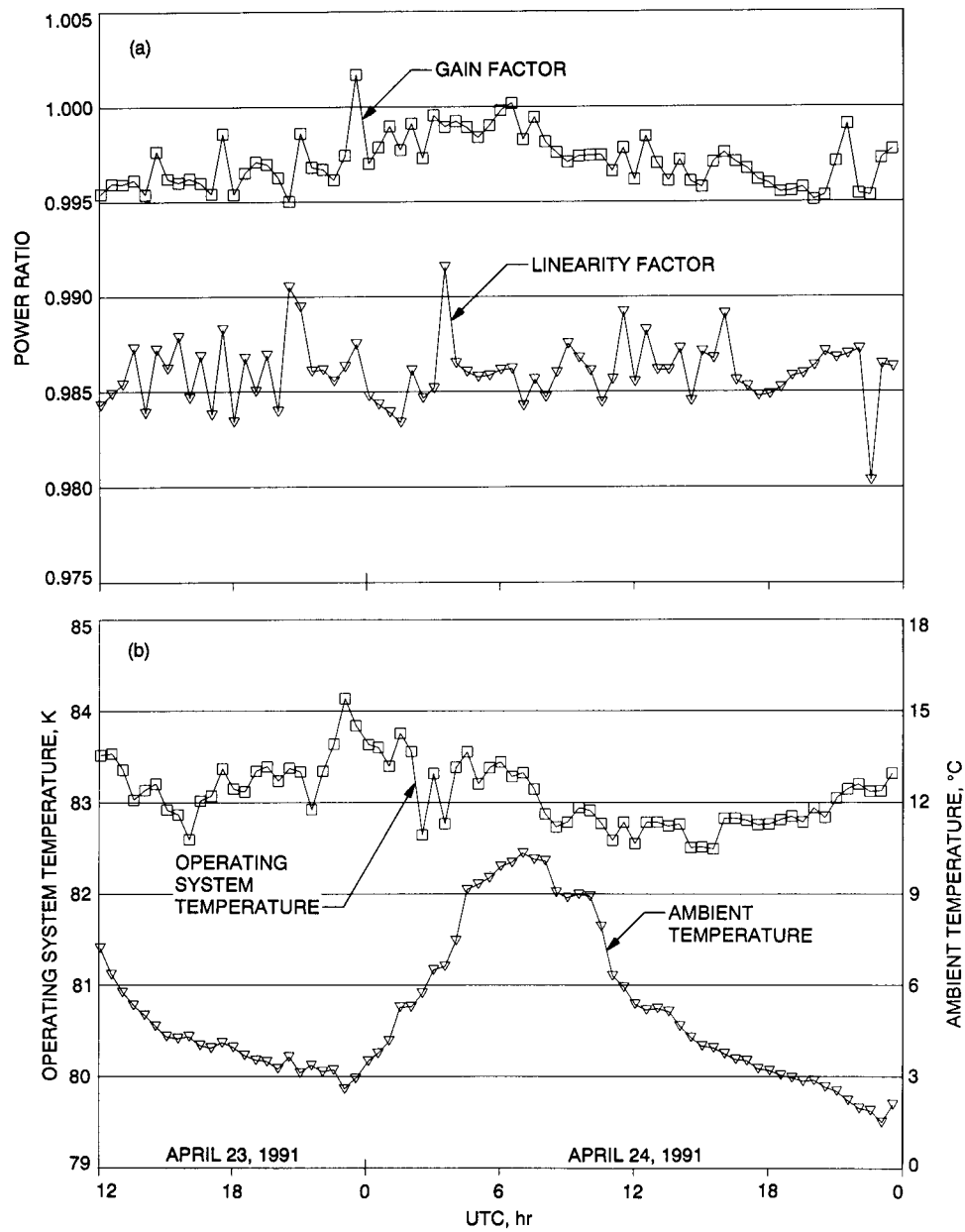


Fig. 10. Ka-band zenith noise-temperature measurements on the ground: (a) system gain and linearity and (b) system temperature.

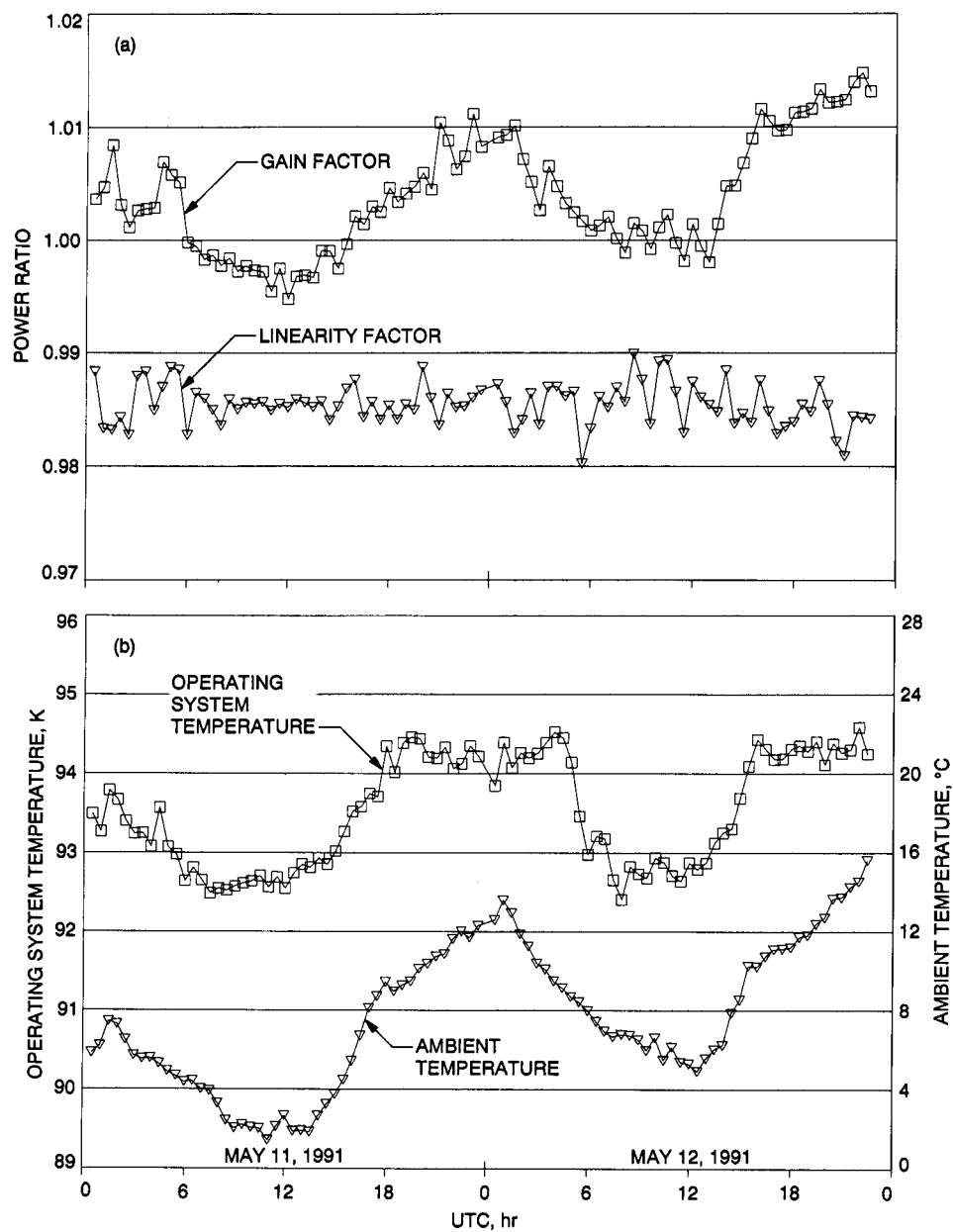


Fig. 11. Ka-band zenith noise-temperature measurements on the antenna: (a) system gain and linearity and (b) system temperature.

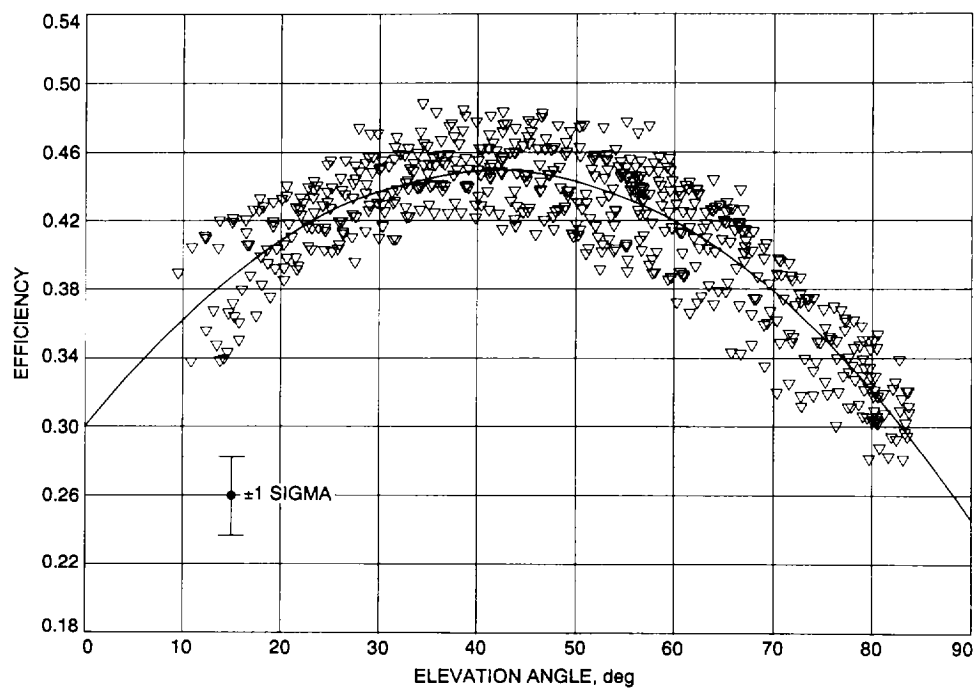


Fig. 12. Plot of Ka-band efficiency.

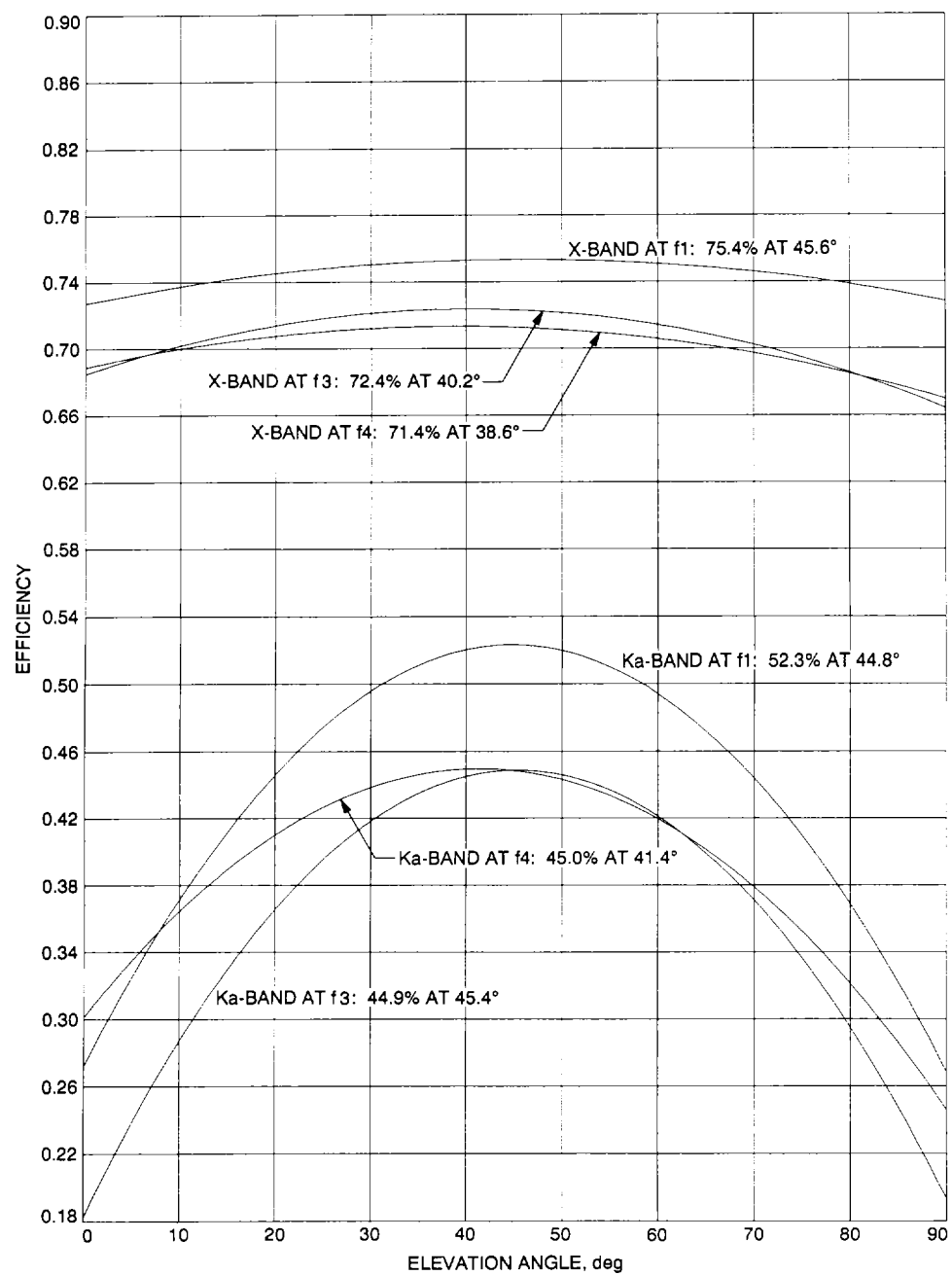


Fig. 13. Comparative results for all of the efficiency measurements on the DSS-13 antenna.